

Impact of electron heat conductivity on electron energy flux

K. Matsuzawa

Advanced LSI Technology Laboratory, Toshiba Corporation
8, Shinsugita-cho, Isogo-ku, Yokohama 235-8522, Japan
E-mail: kazuya.matsuzawa@toshiba.co.jp

Abstract—Equations in the hydrodynamic model were evaluated by direct calculation of the drift, diffusion, and scattering terms obtained by separating the motion of particles in Monte Carlo simulations. It was confirmed that the conservation equations for momentum and energy were constructed adequately. However, it was found that an artificial operation was necessary for describing the energy flux equation. Namely, the parameter of the Wiedemann-Franz law for heat conductivity could be chosen so that the underestimations of the drift and diffusion terms in the energy flux equation cancelled each other. It is shown that this parameter influences the electron temperature in a 50-nm gate nMOSFET.

I. INTRODUCTION

The hydrodynamic model (HDM) [1] has been used to carry out simulation for velocity overshoot and hot carrier effects. In most cases, the system of governing equations in the HDM is constructed by truncating higher order of the divergence term in the energy flux equation [2]–[5] and adjusting the parameter of the Wiedemann-Franz law for heat conductivity to reproduce the physical values obtained by the Monte Carlo (MC) simulation [5]. The validity of the equations has been checked by comparing distributions of physical values such as velocity and energy with those obtained by the MC simulation [6]–[8]. However, the physical values are affected by all terms of drift, diffusion, and scattering. Therefore, it is difficult to distinguish whether or not the expression for each term in the HDM is complete.

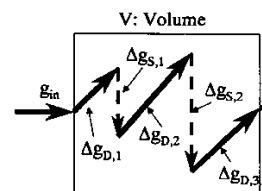
In this paper, each term of the equations in the HDM is calculated independently by separating the motion of particles in MC simulations. A suitable parameter of the Wiedemann-Franz law is evaluated, and it is shown that this parameter can significantly affect the electron temperature.

II. DIRECT MC CALCULATION OF THE BOLTZMANN TRANSPORT EQUATION TERMS

Fig. 1 shows a schematic of the direct MC calculation using changes in a physical value g for each particle in a volume V . The direct MC calculation is performed for the divergence, drift, and scattering, which are the three terms in the moment of the Boltzmann transport equation (BTE) under the steady state condition. The divergence term is obtained by summing all g_{in}^{ip} inflow and g_{out}^{ip} outflow, the drift term is obtained by summing

all the changes $\Delta g_{D,i}^{ip}$ due to the electric field, and the scattering term is obtained by summing all the changes $\Delta g_{S,i}^{ip}$ due to scattering. The divergence term corresponds to the diffusion term in the conservation equation.

Direct calculation of each term



$$\nabla \cdot n \langle \vec{v} g \rangle = \frac{\sum (g_{out}^{ip} - g_{in}^{ip})}{V \Delta t}$$

$$\frac{qn}{m} \nabla \varphi \cdot \left\langle \frac{\partial g}{\partial \vec{v}} \right\rangle = \frac{\sum \sum g_{D,i}^{ip}}{V \Delta t}$$

$$\left(\frac{\partial n \langle g \rangle}{\partial t} \right)_s = \frac{\sum \sum g_{S,i}^{ip}}{V \Delta t}$$

Moment of BTE

$$\underbrace{\nabla \cdot n \langle \vec{v} g \rangle}_{\text{Divergence}} - \underbrace{\frac{qn}{m} \nabla \varphi \cdot \left\langle \frac{\partial g}{\partial \vec{v}} \right\rangle}_{\text{Drift}} = \underbrace{\left(\frac{\partial n \langle g \rangle}{\partial t} \right)_s}_{\text{Scattering}}$$

Fig. 1 Schematic of the direct MC calculation of each term in the moment of the Boltzmann transport equation. Each term can directly be obtained by separating the motion of the particles.

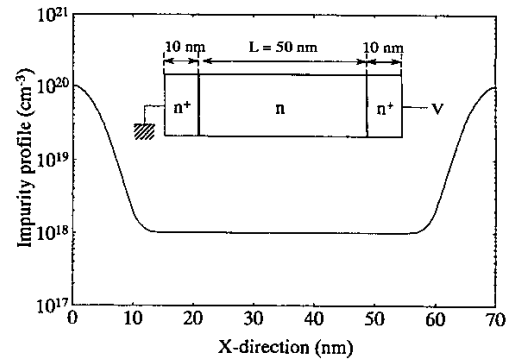


Fig. 2 Impurity distribution in the simulated structure. The inset is a schematic of the device structure.

MC simulations were performed for the n^+nn^+ structure shown in Fig. 2. Figs. 3 and 4 show the distribution of the terms in the conservation equations for momentum and energy under a steady state condition of $V = 0.5$ V:

$$\underbrace{\nabla n m \bar{v}_d}_{\text{Divergence}} + \underbrace{\nabla n k_B T}_{\text{Drift}} - \underbrace{q n \nabla \psi}_{\text{Scattering}} = -n \frac{m \bar{v}_d}{\tau_m}, \quad (1)$$

$$\underbrace{\nabla \cdot \bar{S}}_{\text{Divergence}} - \underbrace{q n \bar{v}_d \cdot \nabla \psi}_{\text{Drift}} = -n \frac{w - w_L}{\tau_w}, \quad (2)$$

where n is the electron density, m the effective mass, \bar{v}_d the average velocity of electrons, k_B the Boltzmann constant, T the electron temperature, q the elementary charge, ψ the potential, τ_m the momentum relaxation time, \bar{S} the energy flux, w the average energy of electrons, w_L the energy corresponding to the lattice temperature, and τ_w the energy relaxation time.

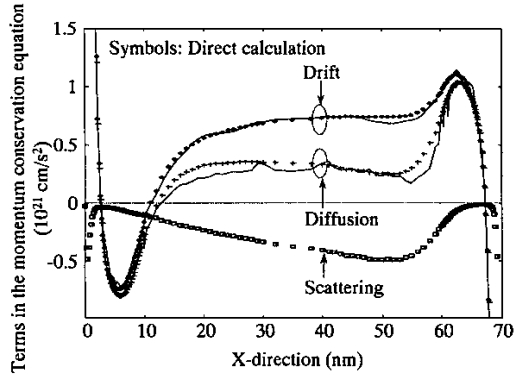


Fig. 3 Distribution of each term in the momentum conservation equation. Each term is adequately expressed by Eqn. (1).

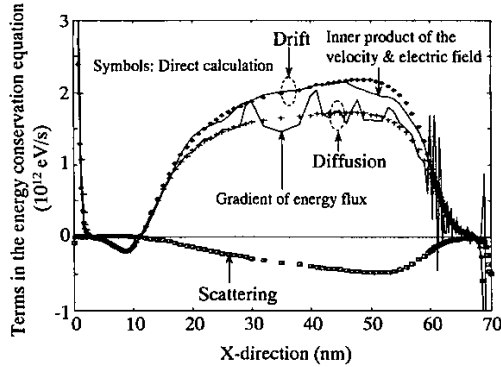


Fig. 4 Distribution of each term in the energy conservation equation. Each term is adequately expressed by Eqn. (2).

The symbols in the figures indicate points obtained by the direct MC calculation outlined in Fig. 1. The momentum conservation equation is derived by substituting $g = \bar{v}$ in the moment equation described in Fig. 1, where \bar{v} is the velocity of each electron and $\bar{v}_d = \langle \bar{v} \rangle$. The energy conservation equation is derived by substituting $g = \bar{\xi}$, where $\bar{\xi}$ is the energy of each electron and $w = \langle \bar{\xi} \rangle$. The solid lines are obtained by

substituting the physical values of n , \bar{v}_d , w , and \bar{S} obtained by the MC simulations into Eqns. (1) and (2). The solid lines agree well with the direct MC calculation. Therefore, the conservation equations for momentum and energy sufficiently describe the transport of momentum and energy. Note that the scattering terms are used to extract the relaxation times as shown in Fig. 5. As is usually expected, the energy relaxation time is larger than the momentum relaxation time and the energy flux relaxation time is almost same as the momentum relaxation time.

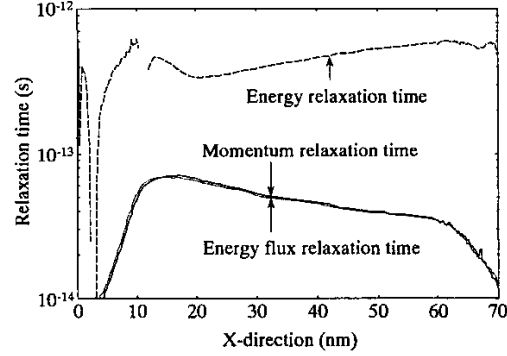


Fig. 5 Distribution of the relaxation times extracted from the scattering rate of physical values. The relaxation times for the energy flux and momentum are almost the same.

III. ENERGY FLUX EQUATION

The distributions of the terms composing the energy flux conservation equation can be obtained as shown in Fig. 6. In this case, $g = \bar{v} \bar{v}^2$, and $\bar{S} = n \langle \bar{v} \bar{v}^2 \rangle$. The drift and divergence terms for the x-direction are derived as follows:

$$\frac{q}{m} n (m v_{dx}^2 + w + k_B T) \frac{\partial \psi}{\partial x},$$

$$\frac{m}{2} (\langle v_{dx}^2 + v_{thx}^2 \rangle (\bar{v}_d^2 + \bar{v}_{th}^2) + 4 v_{dx}^2 \langle v_{thx}^2 \rangle),$$

where v_{dx} is the x-component of the drift velocity, \bar{v}_{th} the thermal velocity, and v_{thx} the x-component of \bar{v}_{th} . The practical equation for \bar{S} can be derived by introducing the relaxation time τ_s and neglecting all the drift energy $m \bar{v}_d^2 / 2$ terms:

$$\bar{S} = \frac{\tau_s}{m} \left[\underbrace{\frac{5}{2} q n k_B T \nabla \psi}_{\text{Drift}} - \underbrace{k_B^2 \left\{ \frac{5}{2} T \nabla n T + \left(\frac{5}{2} + \varsigma \right) n T \nabla T \right\}}_{\text{Divergence}} \right], \quad (3)$$

where τ_s is extracted from the scattering term as shown in Fig. 5, and ς the parameter of Wiedemann-Franz law. In many cases, the assumption of $\varsigma = 0$ has been used because Scharfetter-Gummel discretization can be carried out easily, whereas the value of $\varsigma = -2$ has been determined by Aluru et al. [5] to reproduce MC results.

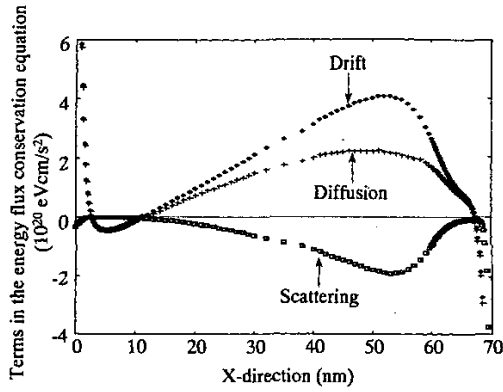


Fig. 6 Distribution of each term in the energy flux conservation equation.

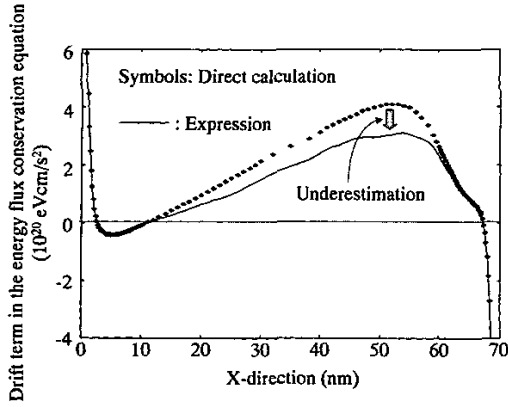


Fig. 7 Distribution of the drift term in the energy flux equation. The drift term is underestimated because the drift energy is ignored in the expression.

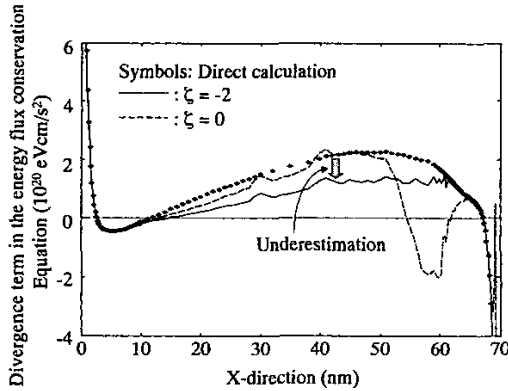


Fig. 8 Influence of the parameter of the Wiedemann-Franz law on the divergence term of the energy flux equation. Ignoring the parameter, that is, setting $\zeta = 0$, causes unnatural undershooting in the high electric field region, whereas underestimation appears in the whole region when ζ is set to -2.

The present direct MC calculation reveals the roles of each term in Eqn. (3). Fig. 7 shows the distribution of the drift term in Eqn. (3). The drift term in the above equation is underestimated relative to the direct MC calculation because all the drift energy components are ignored. Fig. 8 shows the distribution of the divergence term. The result with $\zeta = 0$ shows an irrelevant undershooting in the high field region, whereas the result with $\zeta = -2$ underestimates the divergence term in the whole region. However, as shown in Fig. 9, the energy flux obtained by the direct MC calculation is reproduced well by the expression with $\zeta = -2$. This is because, fortunately, the underestimations in the drift and the divergence terms are cancelled in Eqn. (3).

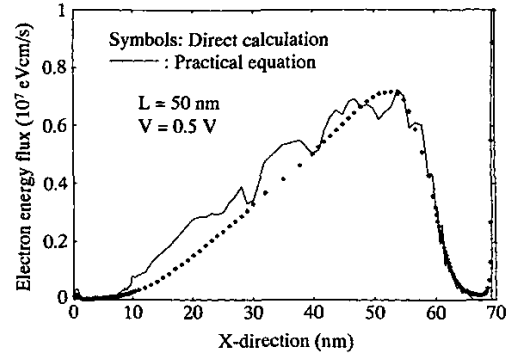


Fig. 9 Distribution of the energy flux for $L = 50$ nm. The practical equation reproduces the result of the direct MC calculation.

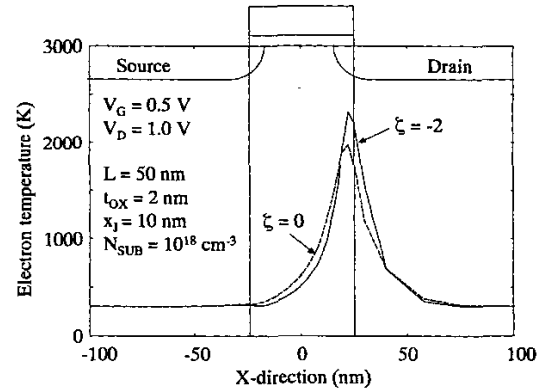


Fig. 10 Distribution of electron temperature at the substrate surface of a 50-nm gate nMOSFET. The electron temperature is significantly affected by the parameter of the Wiedemann-Franz law.

Fig. 10 shows influence of the parameter of the Wiedemann-Franz law on the electron temperature in a 50-nm gate nMOSFET, calculated by extending the Scharfetter-Gummel discretization for Eqn. (3). The parameter value of $\zeta = -2$ causes a reduction of the electron heat conductivity. Therefore, the temperature is concentrated more at the drain depletion region. It is expected that the reduction of

heat conductivity will prevent unnatural heat delays and extreme velocity spikes in the high field region.

Fig. 11 shows the distribution of the energy flux for the case of $L = 100$ nm. The practical equation is thus also applicable to longer channel devices. However, Fig. 12 indicates that the practical equation with $\xi = -2$ might fail in sub-50-nm devices, where the ballistic motion increases. Under such conditions, a higher order equation or a Monte Carlo simulation should be used to predict the carrier temperature more accurately.

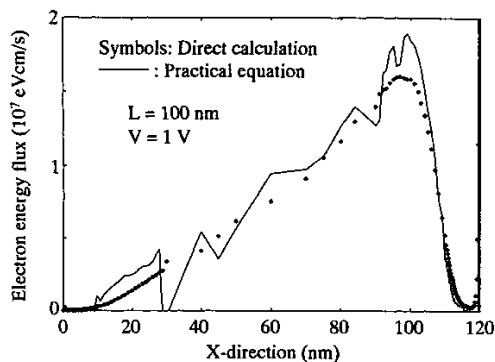


Fig. 11 Distribution of the energy flux for $L = 100$ nm. The practical equation reproduces the result of the direct MC calculation.

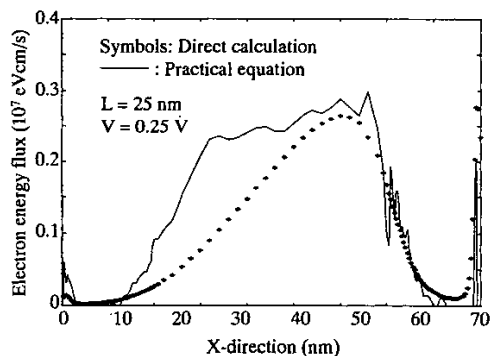


Fig. 12 Distribution of the energy flux for $L = 25$ nm. The practical equation does not reproduce the result of the direct MC calculation. Conservation equations of a higher order or MC simulations might be necessary for sub-50-nm lengths.

IV. CONCLUSION

Each term of the equations in the HDM was calculated by separating the motion of particles in MC simulations to evaluate the validity of the expression for the term independently. It was confirmed that the equations for conservation of momentum and energy reproduce the results of the direct MC calculation. However, it was revealed that the underestimation of the drift term in the energy flux equation has to be canceled by the

underestimation in the diffusion term to reproduce the distribution of the energy flux obtained by the MC simulation. The distribution of the diffusion term in the energy flux was significantly affected by the parameter of Wiedemann-Franz law for heat conductivity. It was also found that an adequate expression for the energy flux is indispensable for accurate prediction of the electron temperature.

ACKNOWLEDGMENT

The author would like to thank Dr. Takagi of the Advanced LSI Technology Laboratory for his helpful suggestions.

REFERENCES

- [1] K. Blotekjaer, *IEEE Trans. Electron Devices*, vol. ED-17, p. 38, 1970.
- [2] A. Pierantoni, P. Ciampolini, A. Liuzzo, and G. Baccarani, *IEICE Trans. Electron.*, vol. E77-C, p.139, 1994.
- [3] W.-S. Choi, J.-G. Ahn, Y.-J. Park, H.-S. Min, and C.-G. Hwang, *IEEE Trans. Computer-Aided Design*, vol. 13, p. 899, 1994.
- [4] P. Golinelli, L. Varani, and L. Reggiani, *Phys. Rev. Lett.*, vol.77, P. 1115, 1996.
- [5] N. R. Aluru, K. H. Law, and R. W. Dutton, *IEEE Trans. Computer-Aided Design*, vol. 15, p. 1029, 1996.
- [6] T. J. Bordelon, X.-L. Wang, C. M. Maziar, and A. F. Tasch, *IEDM Tech. Dig.*, p.353, 1990.
- [7] C. L. Gardner, *IEEE Trans. Electron Devices*, vol. 40, p. 455, 1993.
- [8] S. Ramaswamy and T.-W. Tang, *IEEE Trans. Electron Devices*, vol.41, p.76, 1994.